Optical Fiber Technology 27 (2016) 17–23

Contents lists available at ScienceDirect

Optical Fiber Technology

www.elsevier.com/locate/yofte

Frequency interleave in multicore fiber transmission systems for reducing influence of inter-core crosstalk

S. Okada, K. Igarashi, K. Inoue *

Osaka University, 2-1 Yamadaoka, Suita, Osaka 565-0871, Japan

ARTICLE INFO

Article history:
Received 5 August 2015
Revised 10 November 2015

Keywords:
Multicore fiber transmission
WDM
Crosstalk
Frequency interleave

ABSTRACT

This paper describes a frequency interleaving scheme applied to WDM multicore fiber transmission systems. By shifting channel frequencies between neighboring cores, spectral overlap of inter-core crosstalk channels onto signal channels becomes small, and signal degradation due to the crosstalk is reduced. The effectiveness of the scheme is numerically demonstrated for QPSK and 16QAM signals in a conventional WDM system and duo-binary super-Nyquist WDM systems.

1. Introduction

Wavelength-division-multiplexing (WDM) multicore fiber transmissions are extensively studied to achieve large-capacity transmission over one fiber line [1–8]. In such systems, inter-core crosstalk can cause signal degradation and restrict system performance [6]. To mitigate inter-core crosstalk, Ref. [9] employs a wavelength allocation in which channel wavelengths in one core are interleaved from those in neighboring ones. With that scheme, crosstalk light leaked from other cores does not overlap onto signal lights in the spectrum domain, and signal degradation due to the crosstalk light is avoided. In a previous work, however, the wavelength separation in one core is rather large, so the signal light spectra are fully shifted in neighboring cores; thus, the number of WDM channels per core becomes small. In addition, the effectiveness of the interleaving is not quantitatively evaluated. Another work also employs the wavelength interleaving scheme [10]. However, it aims at mitigating inter-channel nonlinear crosstalk, not linear inter-core crosstalk. The wavelength separation is also rather large, so the signal light spectra in neighboring cores are fully un-overlapped.

In this paper, we apply the frequency interleave scheme to multicore WDM fiber transmission systems with rather narrow channel spacing, in which interleaved signal spectra in neighboring cores partially overlap. Two systems are evaluated: a conventional WDM system with 32-Gbaud and 50-GHz channel spacing, and a duo-binary super-Nyquist system whose channel spacing is narrower than the signal baudrate. A signal format of QPSK or 16QAM is assumed. The effectiveness of the frequency interleave scheme is numerically demonstrated for these systems.

2. System configuration

In this paper, we assume a multicore fiber whose cores are aligned on a single circle as shown in Fig. 1 [6], through which WDM channels are transmitted in each core. The channel frequencies in one core are shifted from those in neighboring cores by half the WDM channel separation, as illustrated in Fig. 1. In this setup, phase-modulated signals, QPSK or 16QAM, are assumed to be transmitted, and then demodulated by digital coherent reception. In coherent receivers, spectral filtering is usually performed at the electrical stage with a bandwidth equal to the signal baudrate, with which noise or crosstalk components within the filtering bandwidth affect the signal demodulation. In our multicore fiber line, crosstalk lights are mainly leaked from neighboring cores whose frequencies are detuned from the signal channel frequency. Thus, the crosstalk components affecting the signal demodulation are expected to be small compared to those in noninterleaving systems; signal degradation due to inter-core crosstalk can then be reduced.

In the following sections, we conduct numerical simulations to evaluate the effect of the above frequency interleave scheme. Two system conditions are examined. One is a conventional WDM system in which 32-Gbaud/s signals are transmitted with 50-GHz channel spacing; i.e., the frequency separation is larger than the signal baudrate. The other is a super-Nyquist WDM system in

* Corresponding author.
E-mail address: kyo@comm.eng.osaka-u.ac.jp (K. Inoue).

http://dx.doi.org/10.1016/j.yofte.2015.11.003
1068-5200/

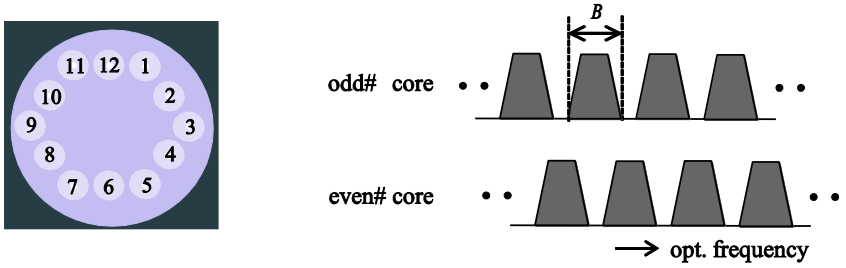

Fig. 1. Core arrangement and channel frequency allocation assumed in our work. *B* is the spectral bandwidth of one signal channel.

which the channel separation is smaller than the baudrate to achieve an ultra-high spectral efficiency.

3. Simulation

3.1. System model

In this work, we employ the simulation model shown in Fig. 2. A transmitter (Tx) launches a phase-modulated signal light onto a transmission line composed of multicore fibers. During the transmission, amplified spontaneous emission (ASE) light from optical amplifiers and crosstalk light leaked from other cores are overlapped onto the signal light. A receiver (Rx) receives and demodulates the transmitted signal suffering from the ASE and the crosstalk lights.

In the transmitter, a pseudo-random bit sequence (PRBS) with a pattern length of 2^{15}–1 is mapped onto the real and imaginary parts of QAM or 16QAM symbols, and then the symbol samples are up-sampled to 2 sample/symbol, for which spectral filtering is performed. The filtered samples are sent to digital-to-analog converters (DACs) followed by an optical IQ modulator (IQM), where the baseband signal is linearly converted to an optical signal. The signal light is then launched to a transmission line. In our simulation, the spectral filtering is assumed to be performed at both the transmitter and the receiver, which forms a designed transfer function in total. Thus, the transfer function of the filtering at the transmitter (or the receiver) is the square root of a designed transfer function. The details of the transfer function are described in the following subsections for each WDM system.

Crosstalk light is created from the above signal transmitter, which is then time-delayed such that data bits are uncorrelated between the signal and the crosstalk; it is then frequency-shifted and phase-rotated such that its phase is uncorrelated to the signal phase. The crosstalk ratio, denoted as Cx and adjusted in each calculation, is defined as the power transfer ratio from one core to a neighboring core. A multicore fiber assumed here has a core arrangement shown in Fig. 1, and we consider crosstalk lights leaked from neighboring cores in our simulations. In evaluating influence of crosstalk in multi-core WDM transmission systems, we consider just the total amount of crosstalk after fiber transmission, and do not specify inter-core crosstalk of a particular fiber or the transmission length, in order to evaluate general properties.

ASE light generated from optical amplifiers is regarded as additive white Gaussian noise (AWGN) [11]. The basic bit error performance – i.e., the baseline – is assumed to be determined by this ASE noise. The signal-to-noise ratio, denoted as SNR and referenced in the following subsections, is defined as the optical power ratio of the signal and ASE within the signal bandwidth.

In the receiver, incoming optical signals are converted to electrical signals by homodyne reception with a local oscillator (LO), which are then down-converted to baseband signals. The linewidths of the LO as well as the transmitters are assumed to be negligible small. This is because we concern crosstalk influence considering spectral filtering effect, and the spectrum broadening due to linewidths of transmitters and an LO laser is negligible small

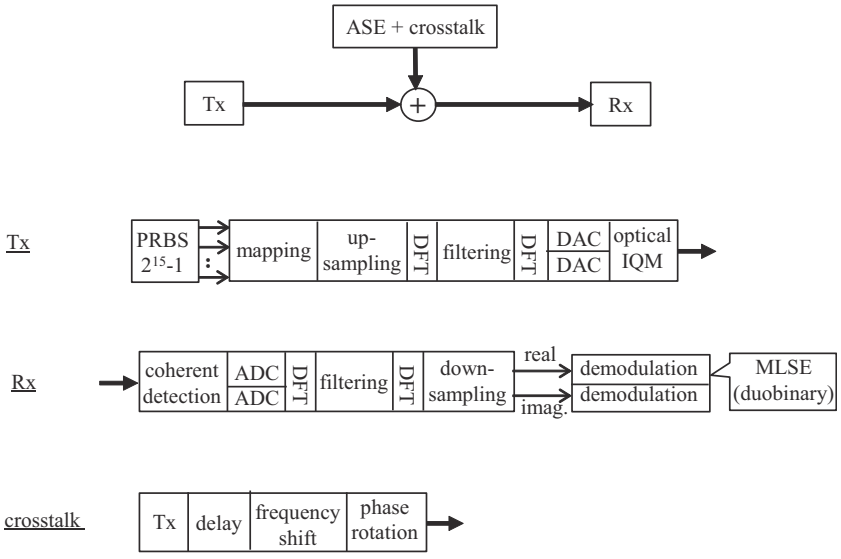

Fig. 2. Simulation model. Tx: transmitter, Rx: receiver, ASE: amplified spontaneous emission, DFT: discrete Fourier transform, DAC: digital-to-analog converter, ADC: analog-to-digital converter, IQM: IQ modulator, MLSE: maximum likelihood sequence estimation.

compared with that due to signal modulation. With the same reason, the relative phase fluctuation between the signal and LO light is assumed to be perfectly compensated, without specifying how to compensation it. The baseband signals are stored by the analog-to-digital converters (ADCs), and the stored samples are spectrally filtered with a transfer function identical to that at the transmitter. The number of samples is 1.2×10^6. The filtered signals are down-sampled, for which bit decisions are made for the real and imaginary parts. In super-Nyquist WDM systems, maximum likelihood sequence estimation (MLSE) is employed in the bit decision process. The necessity of MLSE is described in the following subsection for super-Nyquist WDM systems.

3.2. Conventional WDM system

A 50-GHz spaced 32-Gbaud/s WDM transmission is used in a typical system. We simulate the system performance of this WDM system over a multicore fiber line in this subsection. In evaluating crosstalk influence, the transfer function of the spectral filtering at the receiver is an important parameter to be assumed, because crosstalk components passing through the filtering essentially affect the signal demodulation. In our simulations, we assume cosine-roll-off filtering with a transfer function expressed as

$$F(f) = \begin{cases} 1 & (0 \leqslant |f| \leqslant \frac{B}{4}), \\ \frac{1}{2}\{1 - \sin[\frac{2\pi}{B}(|f| - \frac{B}{2})]\} & (\frac{B}{4} \leqslant |f| \leqslant \frac{3B}{4}), \\ 0 & (0 \leqslant |f| \leqslant \frac{3B}{4}), \end{cases} \quad (1)$$

where f is the frequency and B is the signal baudrate. Note that this transfer function is applied at the transmitter and the receiver in total; thus, the transfer function at the receiver is $\sqrt{F(f)}$.

First, we calculate how the effective crosstalk power after the filtering is reduced by shifting the channel frequencies. The result is shown in Fig. 3, in which the reduction in the effective crosstalk power is plotted as a function of the frequency shift normalized by the channel frequency spacing. The effective crosstalk power is reduced by shifting the channel frequencies as shown in Fig. 3. The reduction is maximized at −2.8 dB when the channel frequencies in one core are at the midpoint between those in neighboring cores – i.e., the frequency-interleaved condition, as illustrated in Fig. 1. This reduction of −2.8 dB in the effective crosstalk is obtained in a 50-GHz spaced 32-Gbaud/s WDM system. For a WDM system with a larger channel spacing, the effective crosstalk reduction is expected to be more enhanced.

The above result regarding the reduction in the effective crosstalk power suggests an improvement of the signal transmission performance by the frequency interleave scheme. However, the crosstalk power reduction does not straightforwardly lead to quantitative evaluation of bit-error-rate improvement. Previous works regarding crosstalk influence on signal quality indicated that in-band crosstalk can be regarded as Gaussian noise when the number of crosstalk lights is large, but not for a small number of crosstalk lights [12,13]. In our systems, crosstalk lights come from just the neighboring two cores; thus, the number of crosstalk lights is small. In addition, the spectra of the signal and crosstalk lights are assumed to be perfectly matched in the previous works, but they are not here. It is not clear in such a situation whether crosstalk degrades the signal as Gaussian noise.

Concerning the above issue, we examine the constellation map at the filter output at the receiver. At the beginning, the constellation of one crosstalk light with no frequency shift is calculated as a reference. The results sampled at the center point of the symbol period are shown in Fig. 4, in which the upper and lower figures are constellation maps and probability densities of the I-component of crosstalk light, respectively. Circular traces are observed in the constellation owing to the condition that the relative phase is random between the signal and the crosstalk lights. The I-component projected from the constellation shows probability peaks at particular points, indicating that the crosstalk light affects the signal much differently from Gaussian noise in this condition.

The probability density shown in Fig. 4(a) can be analytically explained as follows. The constellation map in Fig. 4(a) is actually a circle, whose projection onto the I axis can be expressed as $x = \cos\theta$ (x: position along the I-axis, θ: angle of a position on the circle). From this relationship, we have $dx = -\sin\theta \cdot d\theta = -\sqrt{1-\cos^2\theta} \cdot d\theta = -\sqrt{1-x^2} \cdot d\theta$. Regarding the probability density, on the other hand, $P_X(x)dx = -P_\Theta(\theta)d\theta$ is made, where P_X and P_Θ are probability densities for variables x and θ, respectively. Provided that θ is uniformly distributed, P_Θ is a constant and the equation for the probability densities is rewritten as $P_X(x)dx \propto -d\theta = dx/\sqrt{1-x^2}$, and thus $P_X(x) = 1/\sqrt{1-x^2}$. The profile of the probability density shown in Fig. 4(a) is in accordance with $P_X(x)$.

Fig. 4 shows the results for one crosstalk light. Similar calculations are carried out for our WDM multicore systems, in which crosstalk comes from the neighboring two cores, i.e., two crosstalk lights are independently overlapped onto the signal light. The results for QPSK and 16QAM signals are shown in Figs. 5 and 6,

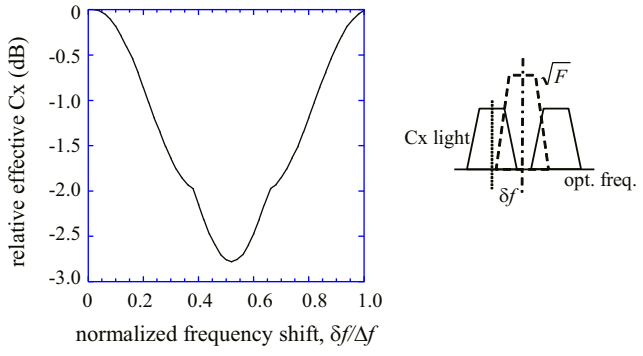

Fig. 3. Reduction in effective crosstalk as a function of frequency shift between neighboring cores. The frequency shift is normalized by channel spacing. Δf is channel spacing and δf is frequency shift.

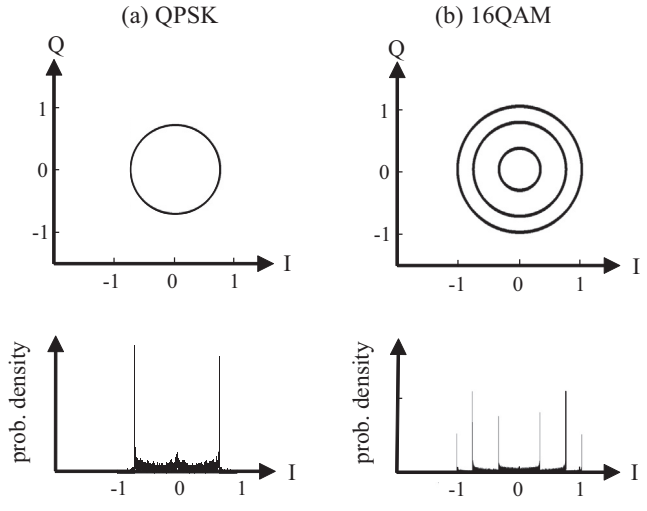

Fig. 4. Constellation (upper) and probability density of I-component (lower) for one spectrum-matched crosstalk light. Signal formats are QPSK and 16QAM in (a) and (b), respectively.

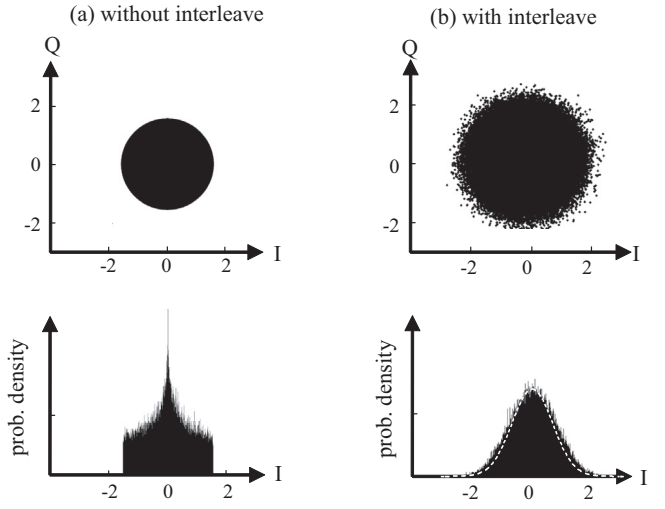

Fig. 5. Constellation (upper) and probability density of *I*-component (lower) of crosstalk from neighboring two cores in conventional QPSK systems with and without frequency interleaving. The white broken line in (b) is a Gaussian curve.

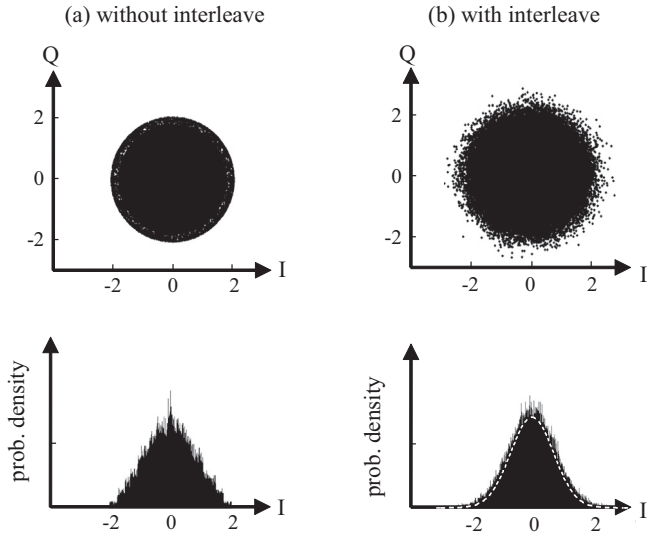

Fig. 6. Constellation (upper) and probability density of *I*-component (lower) of crosstalk from neighboring two cores in conventional 16QAM systems with and without frequency interleaving. The white broken line in (b) is a Gaussian curve.

respectively. The constellation maps are observed to be different from those in Fig. 4 even when the crosstalk light frequency is matched to the signal light frequency, as observed in Figs. 5(a) and 6(a). Accordingly, the probability densities of the *I*-component in Figs. 5(a) and 6(a) are much different from those in Fig. 4, such that one broad peak is observed in the former whereas plural sharp peaks are observed in the latter.

The difference in the probability density (one broad peak in Figs. 5(a) and 6(a) and plural sharp peaks in Fig. 4) can be schematically understood as follows. Fig. 7 respectively plots constellations of two QPSK signals, such that one QPSK signal denoted by the solid line is positioned at the origin $\{I = 0, Q = 0\}$ and another QPSK signal is positioned along the constellation of the first QPSK signal, i.e., the second signal is superimposed onto the first signal. The second QPSK signal denoted by the broken lines is assumed to be positioned at $\{I = 1, Q = 0\}$ or $\{I = 0, Q = 1\}$ or $\{I = -1, Q = 0\}$ or $\{I = 0, Q = -1\}$. This illustration indicates that the symbol point of the total of two QPSK signals concentrate on the origin. As a result,

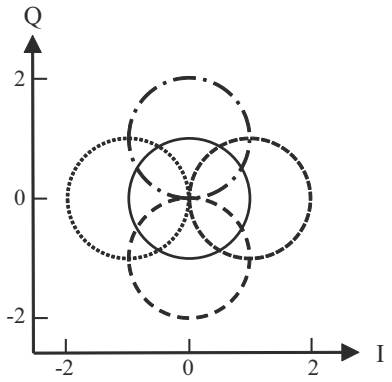

Fig. 7. Constellation when two independent QPSK signals are overlapped. One QPSK signal denoted by the solid circle is positioned such that its center is at $\{I = 0, Q = 0\}$, and another QPSK signal denoted by the broken line is positioned such that its center is at $\{I = 1, Q = 0\}$ or $\{I = 0, Q = 1\}$ or $\{I = -1, Q = 0\}$ or $\{I = 0, Q = -1\}$, i.e., on the solid circle denoting the first QPSK signal with an angle of 0 or $\pi/2$ or π or $3\pi/2$.

the probability density of the *I*-component has one peak at $I = 0$ when two independent QPSK signals are overlapped.

In frequency-interleaving systems, the constellations show noise-like distributions, as shown in Figs. 5(b) and 6(b). This is due to the fact that a fraction of crosstalk passes through the spectral filtering. For reference, a Gaussian profile is overdrawn by the white broken line in the probability density in Figs. 5(b) and 6(b), which is close to the simulation result. The width of the probability density profile looks wider in Fig. 6(b) than in Fig. 5(b). This is because the number of symbol patterns in 16QAM signals is large and the randomness is high as a result, compared with QPSK signals.

The bit error rate (BER) performance is then simulated. The results are shown in Figs. 8 and 9 for QPSK and 16QAM signals, respectively. The definitions of the crosstalk ratio (Cx) and SNR are mentioned in the previous subsection describing our simulation model. For reference, theoretical results calculated by the following equations are also plotted in Figs. 8 and 9;

$$\mathrm{BER}_{\mathrm{QPSK}} = \frac{1}{2} erfc\left(\sqrt{\frac{\mathrm{SNR}}{2}}\right) \quad \text{for QPSK,}$$

$$\mathrm{BER}_{\mathrm{16QAM}} = \frac{1}{2} erfc\left(\sqrt{\frac{\mathrm{SNR}}{10}}\right) \quad \text{for 16QAM,}$$

where *erfc* is the complementary error function. A comparison of the results with and without the frequency interleave, respectively shown in (b) and (a), indicate that the BER performance is improved by interleaving the channel frequencies between neighboring cores.

Finally, in this subsection, the SNR penalty as a function of the crosstalk ratio is calculated, the results of which are shown in Fig. 10. The SNR penalty is defined at a BER of 10^{-3}. It is indicated that the frequency interleave scheme improves the allowable crosstalk ratio by approximately 3 dB for QPSK signals and approximately 4 dB for 16QAM signals.

3.3. Super-Nyquist WDM system

Super-Nyquist WDM transmission systems achieve an ultra-high spectral efficiency, in which the channel spacing is narrower than the signal baudrate [14]. In these systems, the signal channel spectra partially overlap, and inter-channel crosstalk is unavoidable in principle. To reduce the inter-channel crosstalk, duobinary filtering is usually employed [15], whose transfer function is expressed as

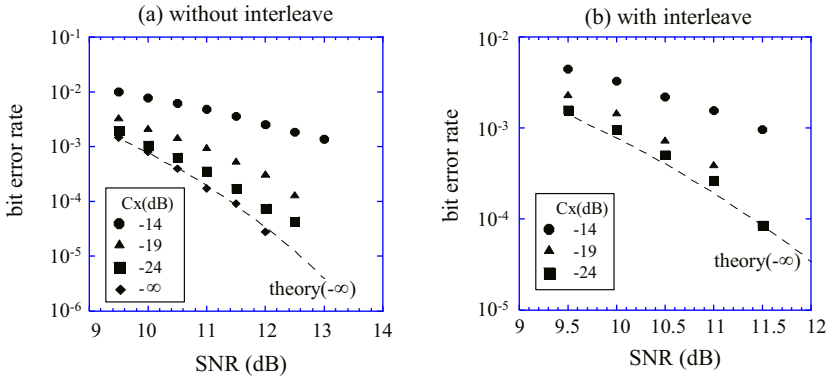

Fig. 8. Bit error rate as a function of signal-to-noise ratio (SNR) for QPSK signal in conventional WDM systems with and without frequency interleave. Cx: crosstalk ratio, SNR: signal-to-noise ratio. Broken line denotes the analytical result with no crosstalk.

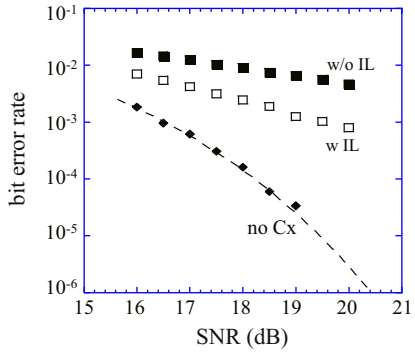

Fig. 9. Bit error rate as a function of signal-to-noise ratio (SNR) for 16QAM signal. Crosstalk ratio is −19 dB. Open and closed squares denote results with and without the frequency interleave, respectively, and the diamonds and broken line denote the simulation and analytical results without crosstalk.

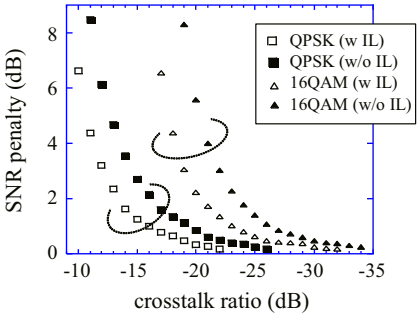

Fig. 10. SNR penalty as a function of crosstalk ratio in conventional WDM systems.

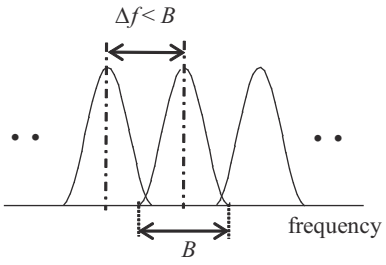

Fig. 11. Signal spectrum in duo-binary super-Nyquist WDM system. B: signal baudrate, Δf: channel frequency separation.

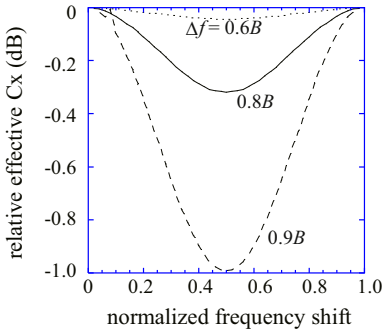

Fig. 12. Reduction in effective crosstalk (Cx) as a function of frequency shift between neighboring cores for duo-binary signal. The frequency shift is normalized by channel separation Δf. The channel separation is $\Delta f = 0.9B$ (broken line), $0.8B$ (solid line), and $0.6B$ (dotted line) where B is the baudrate. Effective crosstalk is normalized by that at no frequency shift, and the frequency shift is normalized by channel separation.

$$F(f) = \begin{cases} \cos\left(\frac{\pi f}{B}\right)\exp\left(\frac{j\pi f}{B}\right) & (|f| \leqslant \frac{B}{2}) \\ 0 & (|f| > \frac{B}{2}) \end{cases}. \quad (2)$$

The duo-binary filtering narrows the signal bandwidth and reduces the inter-channel crosstalk, as illustrated in Fig. 11. However, it has a drawback in which the signal 3-dB bandwidth becomes narrower than the baudrate and inter-symbol interference (ISI) is inherently induced. To mitigate ISI, MLSE is employed in the bit decision processes [16]. In this subsection, we evaluate the effectiveness of the frequency interleave scheme in duo-binary super-Nyquist WDM systems with MLSE.

First, the reduction in the effective crosstalk power by shifting the relative frequencies is calculated. The results are shown in Fig. 12. The effective crosstalk reduction is maximized when the channel frequencies in one core are at the midpoint between those in neighboring cores – i.e., the frequency interleaved condition. The reduction amount depends on the channel separation such that the reduction is small at small separations. This result suggests that the frequency interleave scheme is effective when the channel spacing is close to the signal baudrate in duo-binary super-Nyquist systems.

Next, we examine the constellation map of the crosstalk after the receiver filtering. The results for QPSK and 16QAM signals are shown Figs. 13 and 14, respectively. The channel separation is assumed to be 0.9 times the signal baud rate: $\Delta f = 0.9B$. Compared to the constellations in conventional WDM systems shown in Figs. 5 and 6, the crosstalk components are distributed differently, especially for QPSK signals with no frequency shift, which could be due to the duo-binary filtering effect. In any event, the crosstalk

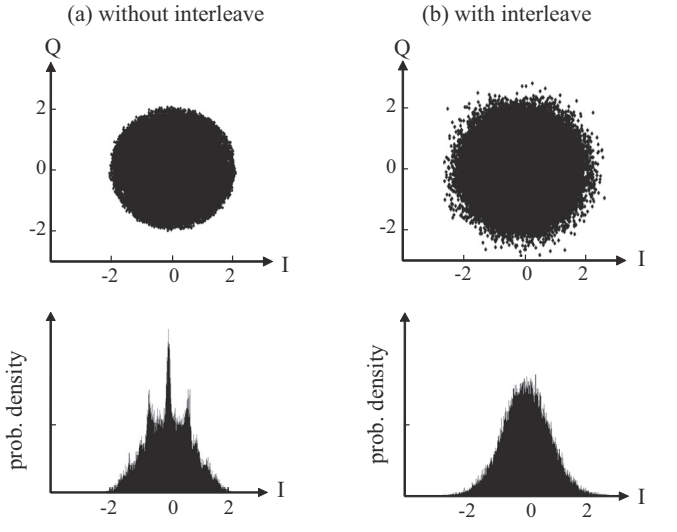

Fig. 13. Constellation (upper) and probability density of *I*-component (lower) of crosstalk from neighboring two cores in duo-binary super-Nyquist QPSK systems with and without frequency interleave. The channel separation is 0.9 times the signal baudrate.

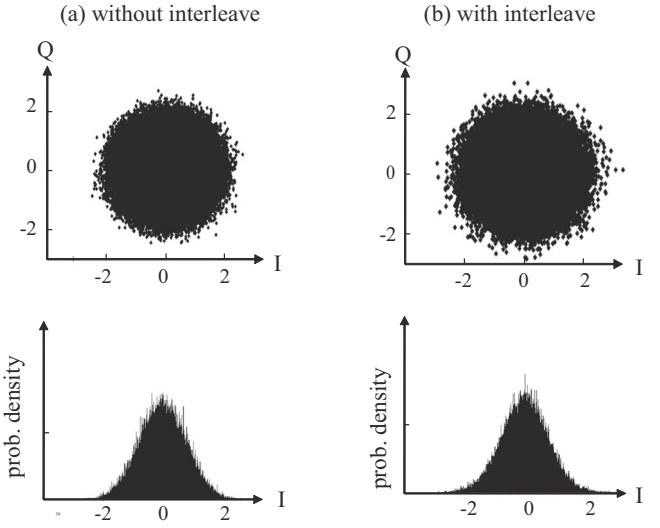

Fig. 14. Constellation (upper) and probability density of *I*-component (lower) of crosstalk from neighboring two cores in duo-binary super-Nyquist 16QAM systems with and without frequency interleave. The channel separation is 0.9 times the signal baudrate.

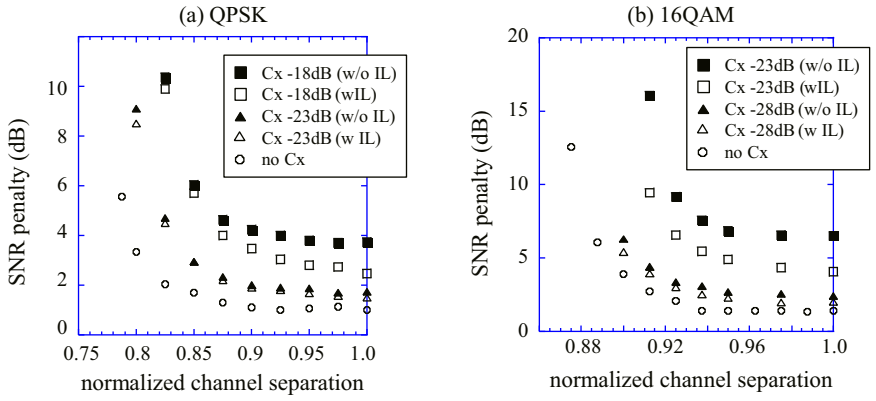

Fig. 15. SNR penalty as a function of channel separation in super-Nyquist WDM systems. Signal format is QPSK in (a), where open and closed squares represent Cx = −18 dB with and without frequency interleave, respectively, and open and closed triangles represent Cx = −23 dB with and without frequency interleave, respectively, and open circles represent Cx = −∞. Signal format is 16QAM in (b), where open and closed squares represent Cx = −23 dB with and without frequency interleave, respectively, and open and closed triangles represent Cx = −28 dB with and without frequency interleave, respectively, and open circles represent Cx = −∞.

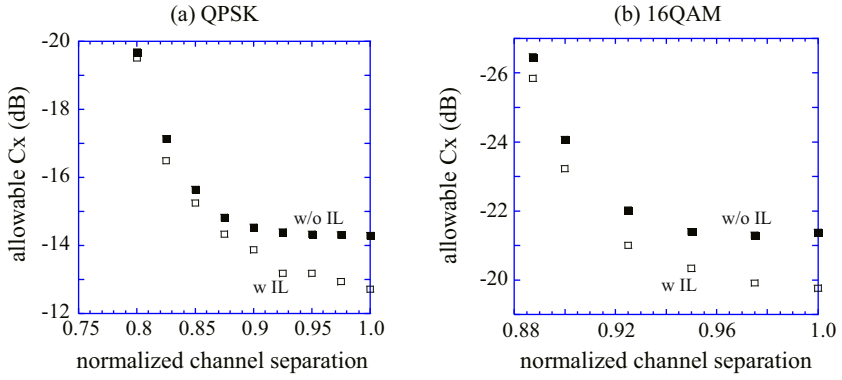

Fig. 16. Crosstalk ratio (Cx) as a function of channel spacing for achieving a BER of 10^{-3}. The channel separation is normalized by the signal baud rate. Open and closed squires denote allowable Cx with and without frequency interleave, respectively.

constellation looks like noise when the frequency interleave is applied.

Next, the BER is calculated as a function of SNR, and the SNR penalty due to inter-core crosstalk at a BER of 10^{-3} is then evaluated from the calculated BER performance. The results are shown in Fig. 15, where the SNR penalty as a function of normalized channel separation is plotted. The SNR penalty is reduced with the frequency interleave for a large channel separation with a low crosstalk ratio. Unfortunately, however, the frequency interleave scheme is not very effective for a narrow channel separation and/or a high crosstalk ratio.

Finally, we examine the effectiveness of the frequency interleave in the ultimate system conditions where the inter-core crosstalk dominantly limits the multicore fiber transmission distance. We assume that the BER is determined by the inter-core crosstalk alone, not by ASE, and estimate the crosstalk ratio to achieve a BER of 10^{-3}. The results are shown in Fig. 16. It is noted that the allowable crosstalk ratio is improved with the frequency interleave scheme at a channel spacing near the signal baudrate. Thus, the effectiveness of the frequency interleave is confirmed in super-Nyquist WDM systems.

4. Summary

A frequency interleave scheme for reducing the influence of inter-core crosstalk in WDM multicore transmission systems was described. By interleaving the WDM channel frequencies between neighboring cores, the effective crosstalk affecting the signal channel is reduced and the signal BER is improved. Numerical simulations confirmed the feasibility of the scheme for QPSK and 16QAM signals in WDM systems with moderate channel spacing and super-Nyquist WDM systems in which the channel spacing is narrower than the signal baudrate.

References

[1] S. Kumar, U.H. Manyan, V. Srikant, US patent 09/852, 173, 2003.
[2] T. Hayashi, T. Taru, O. Shimakawa, T. Sasaki, E. Sasaoka, Opt. Express 19 (2011) 16576–16592.
[3] J. Sakaguchi, Y. Awaji, N. Wada, A. Kanno, T. Kawanishi, T. Hayashi, T. Taru, T. Kobayashi, M. Watanabe, in: The Optical Fiber Communication (OFC2011), Los Angles, US, Mar. 6–10, 2011, Paper PDPB6.
[4] B. Zhu, T.F. Taunay, M. Fishteyn, X. Liu, S. Chandrasekhar, M.F. Yan, J.M. Fini, E. M. Monberg, F.V. Dimarcello, K. Abedin, P.W. Wisk, D.W. Peckham, P. Dziedzic, in: The Optical Fiber Communication (OFC2011), Los Angeles, US, Mar. 8–10, 2011, Paper PDPB7.
[5] J. Sakaguchi, B.J. Puttnam, W. Klaus, Y. Awaji, N. Wada, A. Kanno, T. Kawanishi, K. Imamura, H. Inaba, K. Mukase, R. Sugizaki, T. Kobayashi, M. Watanabe, in The Optical Fiber Communication (OFC2012), Los Angeles, US, Mar. 6–10, 2012, Paper PDP5C.1.
[6] H. Takara, A. Sano, T. Kobayashi, H. Kubota, H. Kawakami, A. Matsuura, Y. Miyamoto, Y. Abe, H. Ono, K. Shikama, Y. Goto, K. Tsujikawa, Y. Sasaki, I. Ishida, K. Takenaga, S. Matsuo, K. Saitoh, M. Koshiba, T. Morioka, in: The European Conference on Optical Communication (ECOC2012), Amsterdam, Netherlands, 2012, Paper Th.3.C.1.
[7] T. Kobayashi, H. Takara, A. Sano, T. Mizuno, H. Kawakami, Y. Miyamoto, K. Hiraga, Y. Abe, H. Ono, M. Wada, Y. Sasaki, I. Ishida, K. Takenaga, S. Matsuo, K. Saitoh, M. Yamada, H. Masuda, T. Morioka, in: The European Conference on Optical Communication (ECOC2013), London, U.K., 2013, Paper PD2.E.4.
[8] K. Igarashi, T. Tsuritani, I. Morita, Y. Tsuchida, K. Maeda, M. Tadakuma, T. Saito, K. Watanabe, K. Imamura, R. Sugizaki, M. Suzuki, in: The European Conference on Optical Communication (ECOC2013), London, U.K., 2013, Paper PD2.E.3.
[9] J. Sakaguchi, Y. Awaji, N. Wada, T. Hayashi, T. Nagashima, T. Kobayashi, M. Watanabe, in: The Optical Fiber Communication (OFC2011), Los Angles, US, Mar. 6–10, 2011, Paper OWJ2.
[10] S.N. Shahi, S. Kumar, Opt. Commun. 294 (2013) 289–293.
[11] K. Inoue, IEEE J. Quantum Electron. 50 (2014) 563–567.
[12] H. Takahashi, K. Oda, H. Toba, J. Lightwave Technol. 14 (1996) 1097–1105.
[13] M.R. Jimenez, R. Passy, M.A. Grivet, J.P. Von der Weid, J. Lightwave Technol. 22 (2004) 942–946.
[14] J.E. Mazo, Bell Syst. Tech. J. 54 (1975) 1451–1462.
[15] J. Li, E. Tipsuwannakul, T. Eriksson, M. Karlsson, P.A. Andrekson, J. Lightwave Technol. 30 (2012) 1664–1676.
[16] J.G. Proakis, M. Salehi, Digital Communications, fifth ed., McGraw-Hill, New York, NY, USA, 2008.